Hindawi
International Journal of Geophysics
Volume 2023, Article ID 9030495, 9 pages
https://doi.org/10.1155/2023/9030495

Research Article

Mt. Etna Tilt Signals Associated with February 6, 2023, $M = 7.8$ and $M = 7.5$ Turkey Earthquakes

Laura Privitera,[1,2] Ferruccio Ferrari,[1] Angelo Ferro,[1] and Salvatore Gambino[1]

[1]*Istituto Nazionale di Geofisica e Vulcanologia, Osservatorio Etneo, Piazza Roma 2, 95123 Catania, Italy*
[2]*Dipartimento di Scienze Biologiche, Geologiche e Ambientali, Sezione di Scienze della Terra, Università di Catania, Corso Italia, 57, 95129 Catania, Italy*

Correspondence should be addressed to Salvatore Gambino; gambino@ct.ingv.it

Received 19 April 2023; Revised 30 November 2023; Accepted 13 December 2023; Published 29 December 2023

Academic Editor: Arkoprovo Biswas

On February 6, 2023, at 01 : 17 UTC, a $M = 7.8$ earthquake struck the southern area of Turkey near Gaziantep town and was followed by a second earthquake of $M = 7.5$ at 10 : 24 UTC with the epicenter in Elbistan city. Both events were associated with the Anatolian Fault System and have claimed over 50,000 victims, as reported by the Disaster and Emergency Management Authority, and caused serious damage in the regions of southern Turkey and northern Syria. Seismic waves related to strong Turkey earthquakes have been recorded both by seismic stations throughout the globe and on other devices such as the ground deformation (GNSS, strainmeters, or tiltmeters) networks. In this paper, we show and analyze the earthquake signals recorded by bore-hole tilt stations that monitor seismic and volcanic activities at Mt. Etna. Tilt stations showed very large variations, despite their distance from the epicenter (approximately 1950 km) with a period between 10 and 25 seconds. We compared tilt and seismic data for a co–located station evidencing a very similar waveform that highlight how tiltmeters respond to translational acceleration rather than ground tilt during a teleseism, suggesting that, for waves with this period, they may behave as horizontal seismometers. By using these signals, we evidence the different behaviors of two of the most used models of tiltmeters on volcanoes (Lily and Pinnacle) and how they are useful for instrument calibration.

1. Introduction

On February 6, 2023, at 01 : 17 : 34 UTC, a $M = 7.8$ earthquake (37.014°E and 37.226°N) was located in Southern Turkey, near the border with Syria, within the known East Anatolian Fault Zone (EAFZ), at a depth of 10 km (USGS, https://earthquake.usgs.gov/). This main event was followed by a vigorous sequence of aftershocks with magnitude between 4.0 and 6.0. Approximately nine hours after the major magnitude event at 10 : 24 : 48 UTC, Turkey was shaken by a second very intense earthquake ($M = 7.5$) with epicenter at 37.196°E and 38.011°N and depth of 7.4 km (USGS, https://earthquake.usgs.gov/; [1, 2]). In Figure 1, we show the locations of the two main events and their focal mechanisms, and we highlight the tectonic structures responsible for the strong seismic release. The East Anatolian Fault (EAF) is a morphologically distinct and seismically active left-lateral strike-slip fault that extends for about 700 km, forming a plate boundary between the Arabian and Anatolian plates in southeastern Turkey. It is a complex of structures whose distribution is highly articulated and complicated, and even today, there is no unambiguous position regarding the real segmentation of the area. The two main earthquakes affected two of the segments in this area: the first event is located in the Main Strand at the Nurdağı-Pazarcik Fault, oriented N60°E and 82 km long; the second one involved the Northern Strand, at the Sürgü Fault (SF), oriented E-W and 55 km long, according to the segmentation proposed by Duman and Emre [3]. In both cases, these are strike-slip faults with a left-lateral source mechanism on a vertical or near-vertical fault, as also evidenced by the focal mechanisms [4] whose characteristics are shown in Table 1.

The occurrence frequency of large earthquakes in Turkey is so high because the forces at play are enormous: plate

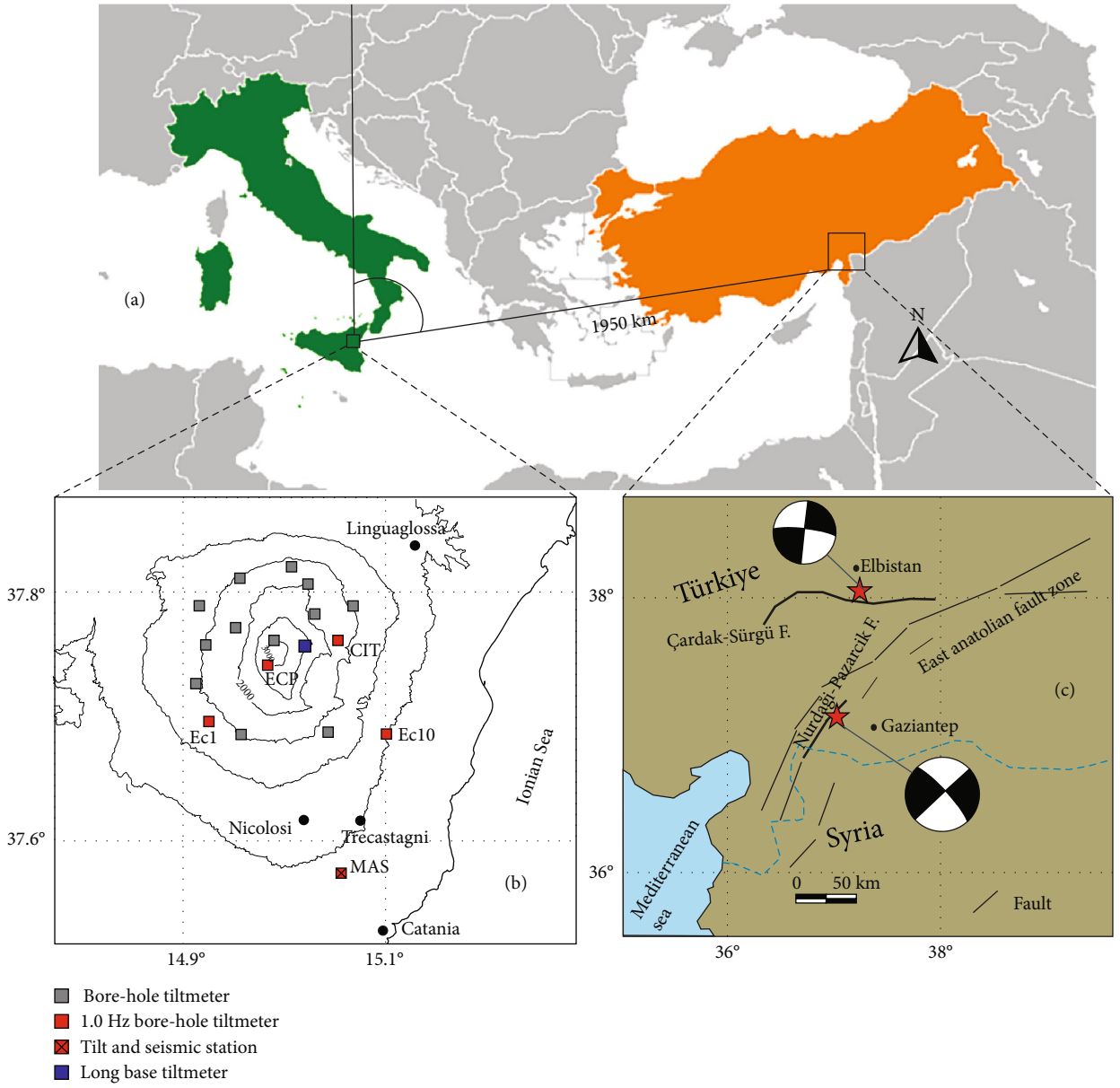

Figure 1: Scheck map of the line-of-sight distance between Mt. Etna and Turkey earthquake area (a). Permanent tilt network of Mt. Etna. The stations with 1 data/sec sampling are shown in red (b). Simplified map of the study region showing the epicentral location and focal mechanisms for both events (c).

Table 1: Focal mechanism parameters [1] (https://earthquake.usgs.gov/earthquakes/eventpage/us6000jlqa/moment-tensor).

	$M = 7.8$				$M = 7.5$		
Plane	Strike	Dip	Rake	Plane	Strike	Dip	Rake
NP1	318°	89°	-179°	NP1	277°	78°	4°
NP2	228°	89°	-1°	NP2	186°	87°	168°

dynamics is dominated by the convergence between the African plate and the Eurasian plate which started as early as the Late Jurassic, around 100 Ma. The continental collision between plates with irregular boundaries caused the formation of microplates and smaller blocks (such as the Arabian block) in relative motion which made the picture even more complex. The differential relative northward motion between the Arabian block and African plate accelerated the convergence of Arabia with respect to Eurasia in the early Pliocene [5], causing the westward extrusion of the Anatolian block, towards the Aegean subduction zone, accommodated by the EAF together with the right-lateral North Anatolian Fault [6–9].

Seismic waves of high-magnitude earthquakes are recorded by the seismic stations which are also installed very distant from the epicenter, and the Earth transmits more efficiently the low-frequency seismic waves (<1 Hz) attenuating the high frequencies. The Turkey earthquake was recorded in Italy also by the Mt. Etna Seismic Network and also on other continuous devices such as strainmeters, gravimeters, or tiltmeters.

The Etneo Observatory (*Osservatorio Etneo*) of the National Institute of Geophysics and Volcanology (INGV-OE) is experienced in measuring continuous ground deformation by using different kinds of instruments. In particular, tiltmeters are a powerful tool for volcano monitoring, providing signals with high precision [10] that accompany eruptive phases and probably identifying eruption precursors [11].

However, bubble tiltmeters, because of their rugged construction and lack of moving parts, are well suited for use as a horizontal seismometer [12]. A joint analysis of seismic and tilt data has shown that, for the teleseism frequency band, the observed tilt signal is not related to the ground tilt but to translational ground acceleration caused by body and surface waves passing [13]. Moreover, teleseismic waves recorded with a co–located seismometer and bubble tiltmeter may be used to determine the response of the tiltmeter [14]. The reasons for using tiltmeter measurements for teleseisms are to define the behavior of the widespread borehole tiltmeter models adopted to low-frequency signals and how these signals may be used to verify the tiltmeter orientation. Similar investigations have been achieved on tiltmeters worldwide, as in the Kamchatka Peninsula (Russia) [15], Chateau Observatory (New Zealand) [13] and Mount St. Helens (USA) [14].

This work presents results of tilt recording at five different stations of the February 6, 2023, $M = 7.8$ and $M = 7.5$ Turkey earthquakes and analyses of the simultaneous recording of the two earthquakes to a co–located tiltmeter and seismometer.

2. Tilt Network

Continuous tilt measurements are used for ground deformation monitoring in many active volcanic areas in the world [16] and are usually used to record middle-short-term eruption precursors (e.g. [17]). Tiltmeter data may also be used for local and regional earthquake source studies. Fault activation causes both seismic waves which induce transitory tilt as they pass through (e.g., [14]) and ground deformation which is recorded as permanent offsets on tiltmeters. The amplitude of permanent changes is related to the source-station distance and fault slip features which are useful for putting constraints in fault source studies (e.g., [18–21]). For large distant events such as a teleseism, the permanent variation is generally negligible.

A tiltmeter is a device that measures changes in the local tilt of the Earth's surface; the instruments that allowed obtaining high-precision measurements may be grouped in a short base that uses a bubble or a pendulum sensor and a long base that uses the free surface of a liquid as a horizontal reference [22].

Borehole bubble tiltmeters represent the most common technique used on volcanoes [16] that uses the electrolytic bubble sensor that was first described by Cooper [23]. The principle is that of a bubble in an electrolytic fluid inside a small disk of a few centimeters; when the instrument tilts, the liquid moves around the bubble, and the electrodes sense changes in resistance as the surface covered by the conductive liquid decreases on one side and increases on the other. A circuit converts these changes to DC signals that are linearly proportional to angular rotation [24]. To determine the tilt direction, the instrument has two single-axis sensors, perpendicular to one another. The electrolytic bubble tilt sensors may be mounted on a platform housing but generally are inserted in a cylinder for installation in a borehole (Figure 2).

Tilt systematic monitoring has been carried out on Mt. Etna by the INGV-OE from the late 1970s, by using bubble borehole tiltmeters [25, 26]. Up to the early 2000s, signals from tiltmeters (AGI Mod 722 and Mod 510) in holes between 2 and 4 meters deep were affected by environmental noise (e.g., [27]).

Starting from 2007, we further installed deep stations (from 10 to 30 meters) using high-resolution (10^{-8}–10^{-9} radians) self-leveling instruments with onboard magnetic compasses. Currently, Mt. Etna tilt network also comprises three summital stations installed at a depth of 27-30 meters [28]. All these installations are characterized by constant temperature with low noise; this allows even the detection of tilt tides [10].

Two types of instruments are used: the Lily model by AGI/Jewell and the Pinnacle 5000 Series by Pinnacle/Halliburton, each consisting of a stainless steel cylindrical body measuring 64 mm in diameter for the Pinnacle 5000 Series and 51 mm for the AGI/Jewell Lily which contains two tilt sensors at the base placed orthogonally to each other, a thermometer, and a solid-state magnetic compass sensor. In order to level the instruments, a motorized system enables tilting the sensors. The borehole tiltmeters have a flat response to ground tilt above a period of 3 sec; however, the Pinnacle model uses a 30 sec low-pass filter intended to reduce high-frequency noise (Figure 2).

The Mt. Etna permanent tilt network (Figure 1(b)) currently comprises 18 biaxial instruments installed in shallow boreholes and one fluid (mercury) long-base instrument set inside two 80 m long tunnels at the Volcanological Observatory of Pizzi Deneri [11].

At present, most of the stations are programmed for 1 data/min, including acquisition of tilt, air, and ground temperatures; air pressure; and instrumental control parameters considering this configuration is appropriate for detecting the ground deformation signals related to volcanic activity. On November 2022, five stations in the network were also programmed for faster acquisition (1 data/sec), and these stations (Table 2) have been used in this paper to analyze the February 6 earthquakes.

3. Tilt Data

The February 6, 2023, $M = 7.8$ and $M = 7.5$ Turkey earthquakes caused very large changes on tiltmeters (Figure 3)

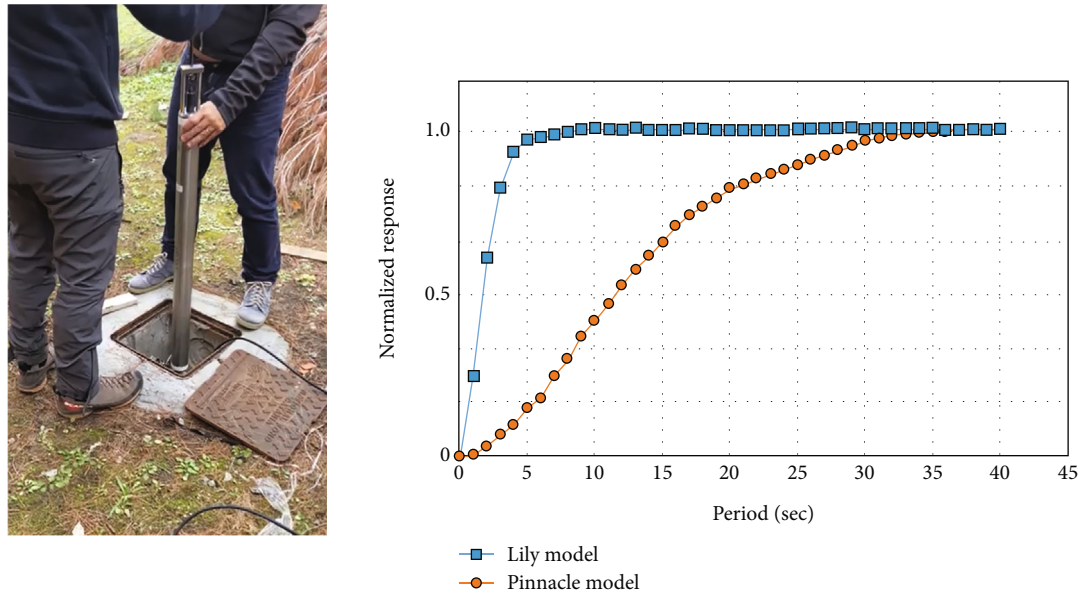

Figure 2: Installation phase of a bore-hole cylindrical tiltmeter and response curves of the two sensors (Lily and Pinnacle models) used on the Mt. Etna network.

Table 2: List of the tilt stations with 1 Hz sampling.

Station	Name	Instrument and depth	Latitude	Longitude	Elevation	Tilt_X orient.
FAR	Contrada Farelle	Lily 10 meters	37.692	15.083	1017	N78°E
MAS	Mascalucia	Lily 30 meters	37.580	15.052	450	N272.5°E
ECP	Cratere del Piano	Pinnacle 30 meters	37.744	14.987	3010	N194°E
EC1	Case Ventura	Lily 10 meters	37.703	14.935	1480	N122°E
CIT	Rifugio Citelli	Lily 10 meters	37.760	15.060	1740	N239°E

exhibiting signals with characteristics identical to seismic sensors with the presence of P and S waves followed by larger surface waves (Love and Rayleigh). In particular, the MAS station showed the largest variation with 150-200 microradians peak to peak for the first event and larger values for the second; FAR, CIT, and EC1 recorded values of 100-150 microradians and 30 microradians for ECP (Figure 3); a first consideration is that the $M = 7.5$ signals showed greater amplitudes than those of $M = 7.8$, probably due to the alignment between the instrument direction and the strike of the $M = 7.5$ fault.

We rotated the tilt data into global N-E coordinates and directly compared the time series recorded at the different stations, obtaining signals very similar to those of stations equipped with the same tiltmeter model (Lily) despite being at different distances from the earthquakes' epicenters. ECP, which instead uses the Pinnacle model, showed a higher frequency filtered signal due to its internal filter (Figure 4).

Spectral components show a frequency between 0.04 and 0.1 Hz (10-25 sec), and obviously, ECP shows a predominant low frequency and a minor component at 0.4-0.5 Hz typical of Mt. Etna LPs whose presence is obliterated by the strong variations of teleseism.

4. Simultaneous Recording on a Co–Located Tiltmeter and Seismometer

The permanent seismic network located on Mt. Etna consists of about 30 digital broadband 3-component stations [29]. The February 6, 2023, $M = 7.8$ and $M = 7.5$ seismic events had been recorded by all the stations about 4 minutes later (01 : 21 : 30 UTC and 10 : 28 : 30 UTC, respectively) with respect to origin time with very high amplitudes. The waves generated by these earthquakes affected our stations for a duration of about 3-4 hours for each event. The teleseismic waves include P, S, and surface waves that typically appeared most strongly in the records (Figure 5).

Of the five tilt stations, two coexist with seismic stations (ECP and MAS); however, the ECP summit seismic station was not functioning in February, and therefore, we have taken into consideration the signals of the co–located station of MAS (Figure 1) for comparison. Seismic and tilt instrumentations are installed in the same site (37.5791-15.0526 and altitude of 450 m), and the seismic station uses a Guralp CMG 3EX broadband sensor at 120 s. The first 10 minutes of the three components' seismograms of the two events ($M = 7.8$ and $M = 7.5$) are reported in Figure 5 with particle

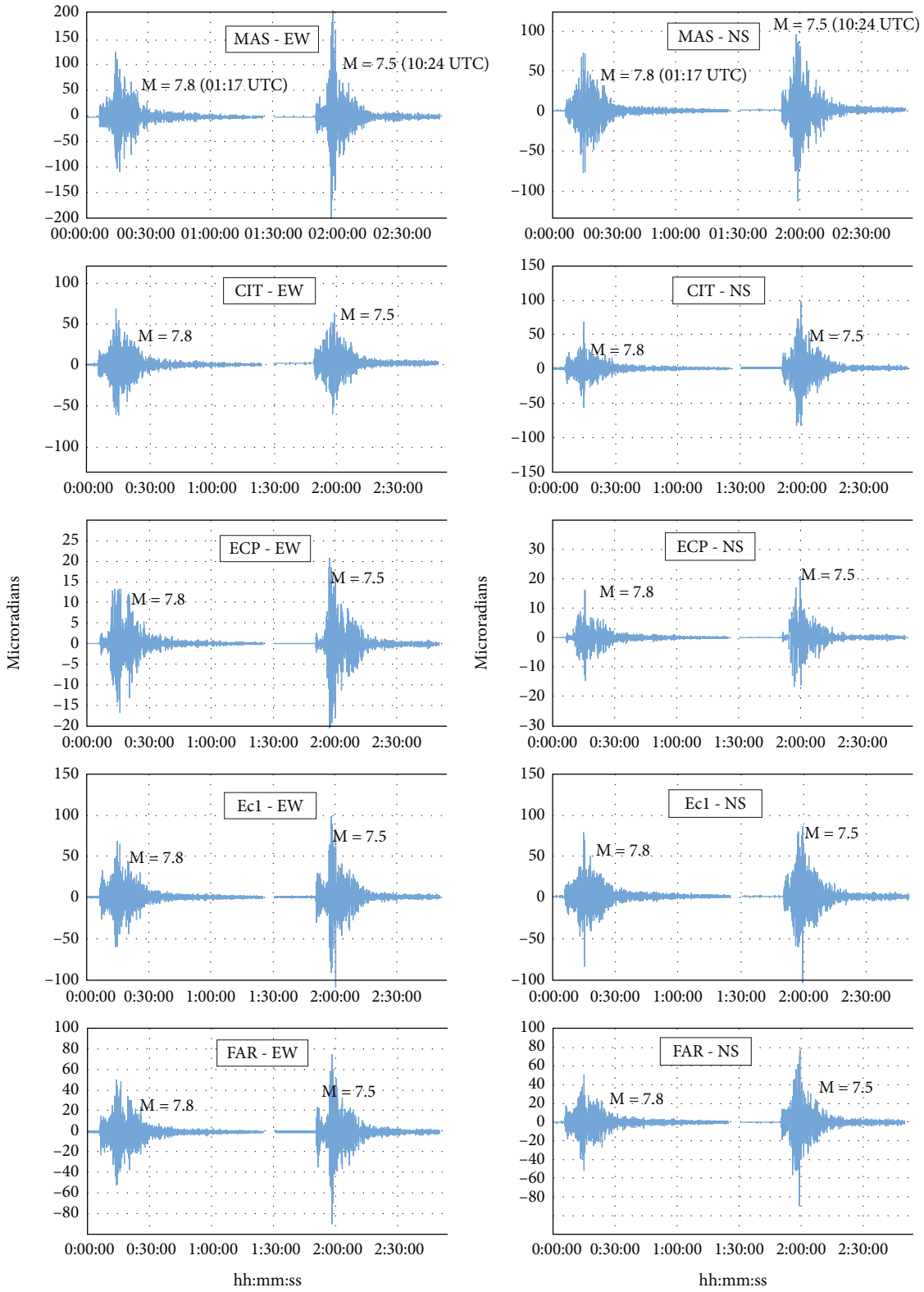

Figure 3: Tilt recorded at the 1 Hz station during the two main Turkey earthquakes.

motion of NS versus EW that evidences a seismic wave front direction of about N80°E for both events.

We derived and converted the velocity signal in order to obtain acceleration in m/s^2 that we compared with NS and EW tiltmeter components that we rotated by using the instrument compass angle of N272.5°E obtaining a strong similarity in the waveforms and amplitude with cross-correlation coefficients between 0.93 and 0.96 (Figure 6).

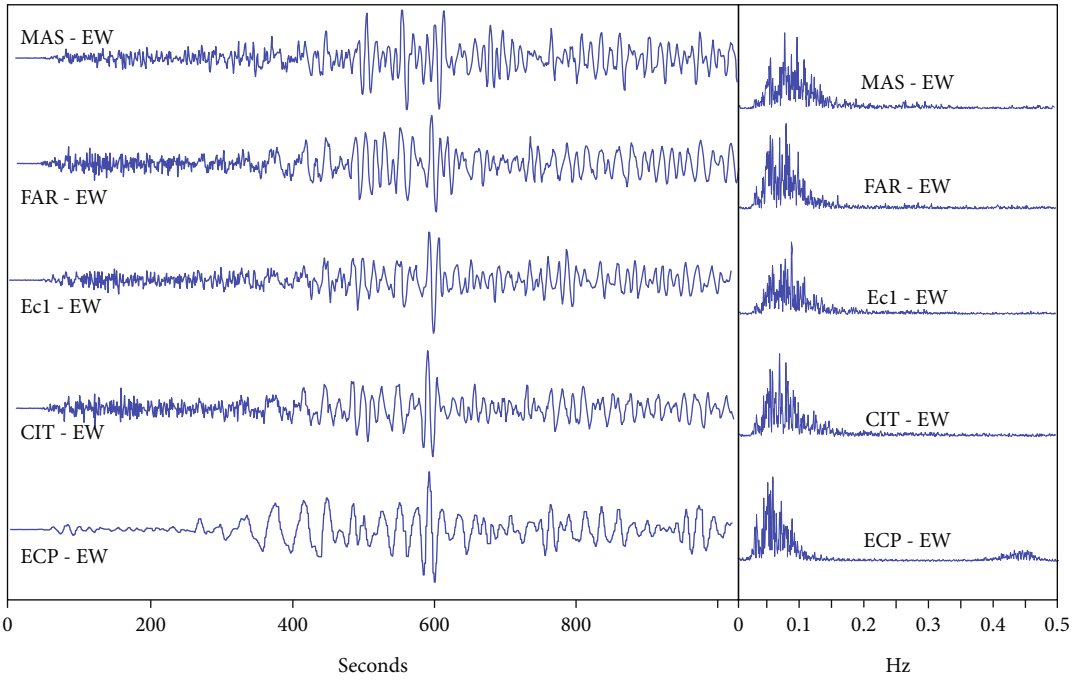

Figure 4: EW-tilt component recorded at the five stations and related spectra.

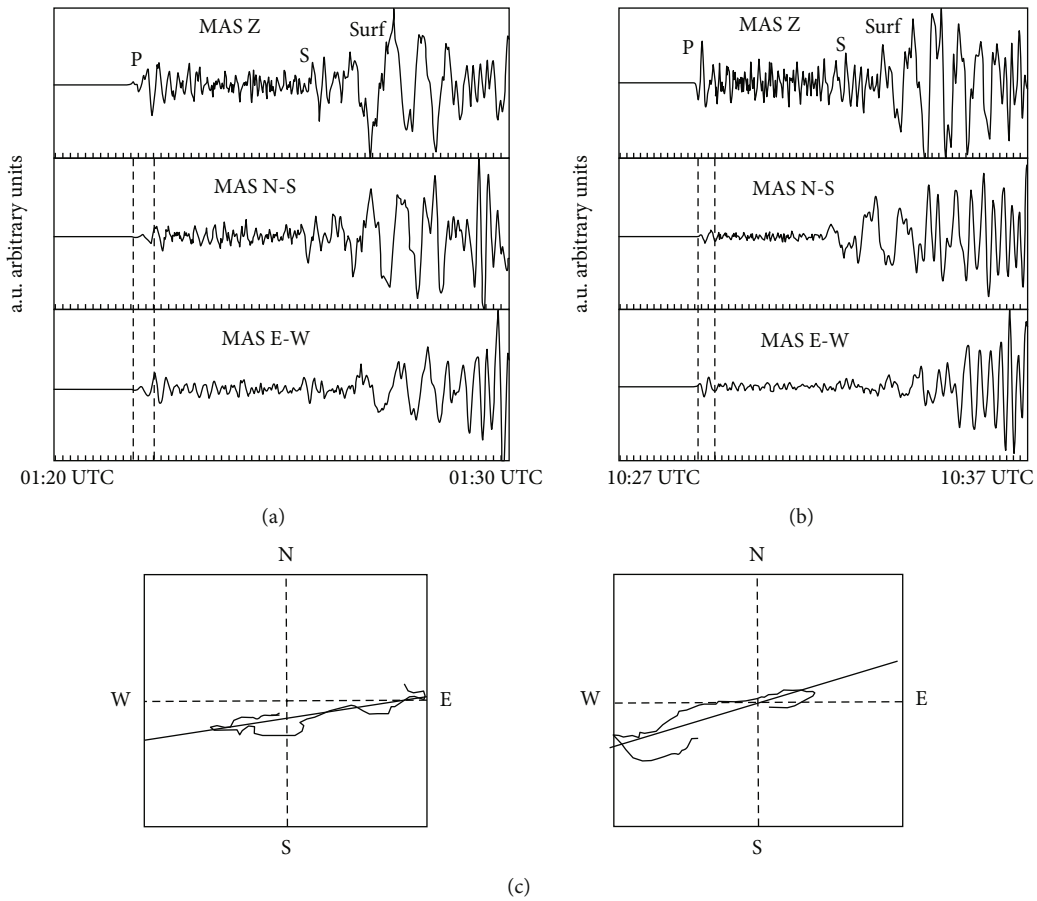

Figure 5: Seismograms of first 10 minutes of the $M = 7.8$ and $M = 7.5$ events (a, b). Particle motion of NS versus EW components that evidences the seismic wave front direction (c).

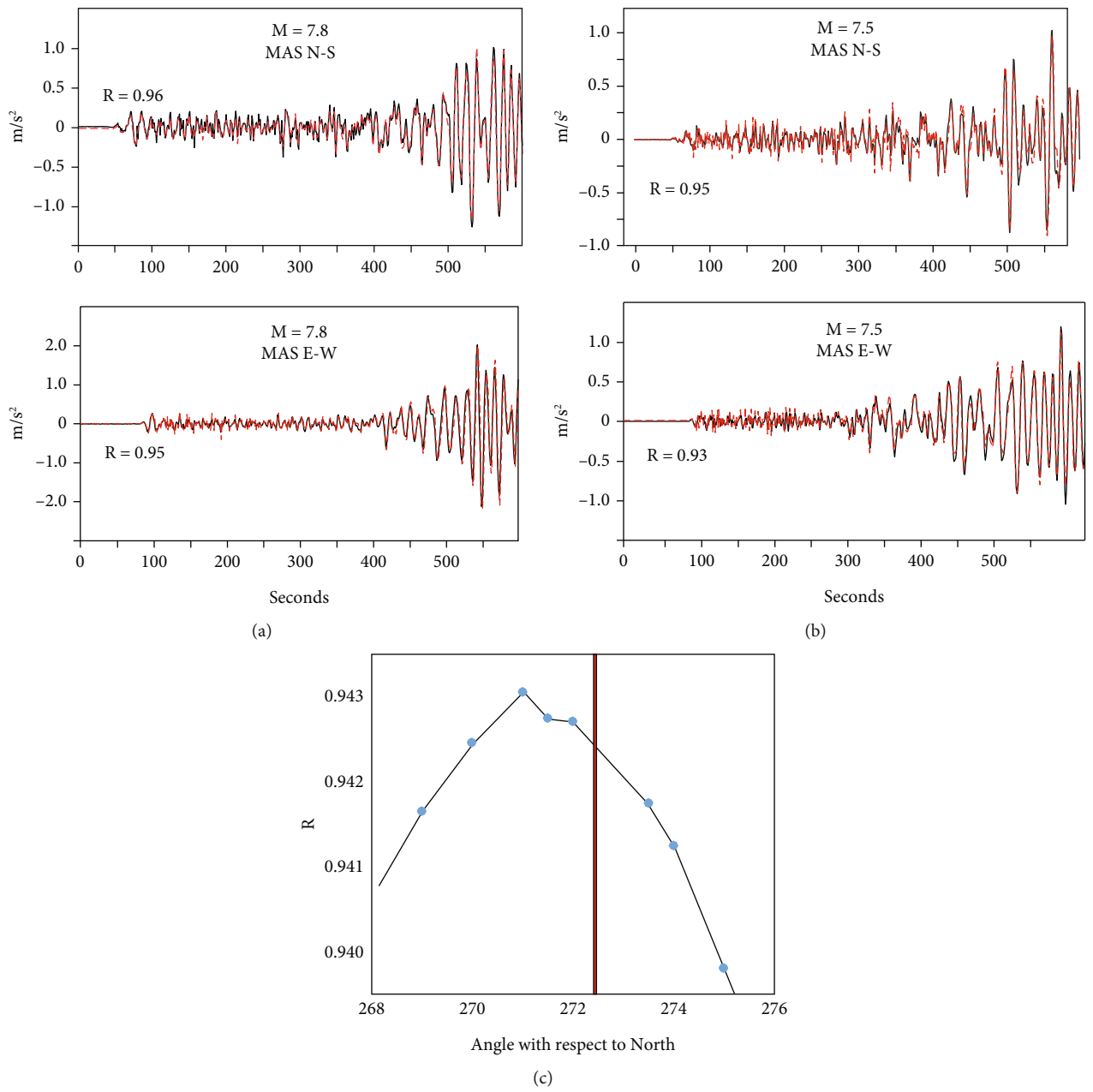

Figure 6: Comparison of the observed horizontal seismic acceleration (grey) with the observed tilt contribution (red) and related correlation coefficient R for the NS and EW components, respectively, for the two events (a b). Graph of mean R obtained on EW and NS for the $M = 7.5$ with respect to angle rotation of the tilt components (c). The red line is the compass angle.

We also verified the orientation of the MAS tiltmeter changing the angle rotation of the components and compared them with the seismic data in order to obtain the best cross-correlation coefficient. We obtained a value of N271°E as the best result, only approximately 1.5 degrees of difference with respect to the compass angle (Figure 6(c)).

5. Discussion and Conclusions

This work analyzes the signals of the strong Turkey earthquakes recorded by bore-hole bubble tilt sensors. Tiltmeters recorded very high variations with a period of 15-20 sec, and amplitude differences recorded at the various stations reflect the site responses (e.g., [30]) while the ECP station evidenced the effect of the 30 Hz filter mounted on the Pinnacle instrument which was not present on the AGI/Jewell Lily which had a flat response since 0.3 sec.

It was evident that the signals of the $M = 7.5$ earthquake showed greater amplitudes particularly for surface waveforms, with respect to the $M = 7.8$ earthquake as a result of different focal mechanisms. Indeed, it is well known that relative amplitudes are strongly dependent on the orientation of the observer with respect to the fault plane of the earthquake owing to the radiation pattern of the P and Rayleigh waves [31].

However, the large changes recorded should not be attributable to variations in the inclination of the ground but to transient ground acceleration, as for periods of 2-20 sec, they behave as horizontal seismometers [12].

This means that the observed tilt (ϕ_{obs}) is an apparent tilt signal, whose amplitude equals the observed seismic horizontal acceleration (a_{obs}) that is a translational ground acceleration. Theoretically, for a propagating wave of a far-field event, the ratio of deformation to acceleration on the tiltmeter signal can be approximated to g/fv with $f = 1/T$ the wave frequency and v the velocity wave phase [32]. For the Turkey events, where $T \sim 15 - 20$ s and $v \sim 3000\ \mathrm{m\,s^{-1}}$, this ratio is ~0.06, and the tiltmeter signal should therefore be dominated by acceleration as evidenced by Fournier et al. [13] suggesting the follow relationship:

$$\phi_{obs} = \frac{a_{obs}}{g}. \quad (1)$$

By using this relationship, we considered the rotated tilt data of a co–located station (MAS) into N-E coordinates and directly compared the time series with the derivative seismic data for the two events and both directions (NS and EW) obtaining a very good agreement in both waveforms and amplitude, with very high correlation coefficients of 0.93 and 0.96, respectively. High correlation values (0.81 and 0.78) have also been found by Fournier et al. [13] for the same instrument model (Lily by AGI/Jewell) installed in New Zealand for a teleseism, 550 km away from the station.

The use of teleseismic data is a good tool for verifying the absolute orientation of the tilt sensors, as well described by Anderson et al. [14] for the Mount St. Helens tilt network. In the MAS station case, we evidenced a very small difference (1.5 degrees) in its orientation with respect to tiltmeter compass information. Moreover, the similarity in signals recorded at the four stations with the same instruments (AGI/Jewell Lily) suggests that orientations obtained by a compass are mostly correct.

Finally, this analysis has allowed us to determine that for a far-field event with a period of 10–25 s, tiltmeters recorded only translational acceleration. However, Mt. Etna is a volcano that normally generates LP (*long period*) events with periods of about 2 s and, in specific periods, VLP (*very long period*) events characterized by periods of 10–20 s similar to those of teleseisms [33]. LP events are seismovolcanic signals linked to the magmatic fluid dynamics, and their variations over time are used to understand eruptive dynamics. No VLP events have been recorded since the five stations were programmed for faster acquisition; however, a possible study of VLP tilt recording poses the problem of verifying the tilt contribution and acceleration in order to avoid that the signals recorded by bubble tiltmeters may be misinterpreted.

Data Availability

The data used to support the findings of this study are available from the corresponding author upon request.

Conflicts of Interest

The authors declares that they have no conflicts of interest.

Acknowledgments

We are indebted to INGV-OE technicians who ensured the regular working of the tilt and seismic network. This research has been financially supported by "PON-GRINT" and "SiC nano for PicoGeo" projects.

References

[1] D. Melgar, T. Taymaz, A. Ganas et al., "Sub- and super-shear ruptures during the 2023 Mw 7.8 and Mw 7.6 earthquake doublet in SE Türkiye. Submitted at Seismica," 2023, https://www.researchgate.net/publication/368680344.

[2] P. Somerville and J. Evans, "Cause and surface faulting of the Turkiye earthquakes of February 6, 2023. Briefing Note, 478. February 16, 2023," 2023, https://riskfrontiers.com/insights/turkey-earthquakes-cause-surface-faulting-2023/.

[3] T. Y. Duman and Ö. Emre, "The East Anatolian Fault: geometry, segmentation and jog characteristics," *Geological Society, London, Special Publications*, vol. 372, no. 1, pp. 495–529, 2013.

[4] USGS, "Earthquake hazards program," 2023, https://www.usgs.gov/programs/earthquake-hazards/earthquakes.

[5] E. Bozkurt, "Neotectonics of Turkey - a synthesis," *Geodinamica Acta*, vol. 14, no. 1-3, pp. 3–30, 2001.

[6] J. F. Dewey, M. Hempton, W. S. F. Kidd, and F. Şaroğlu, "Shortening of continental lithosphere: the neotectonics of Eastern Anatolia - a young collision zone," *Geological Society, London, Special Publications*, vol. 19, no. 1, pp. 1–36, 1986.

[7] J. Jackson and D. McKenzie, "Active tectonics of the Alpine–Himalayan belt between western Turkey and Pakistan," *Geophysical Journal International*, vol. 77, no. 1, pp. 185–264, 1984.

[8] D. McKenzie, "Active Tectonics of the Mediterranean Region," *Geophysical Journal International*, vol. 30, no. 2, pp. 109–185, 1972.

[9] D. McKenzie and C. Bowin, "The relationship between bathymetry and gravity in the Atlantic Ocean," *Earth and Planetary Science Letters*, vol. 81, no. 11, pp. 1903–1915, 1976.

[10] A. Ferro, S. Gambino, S. Panepinto, G. Falzone, G. Laudani, and B. Ducarme, "High precision tilt observation at Mt. Etna volcano, Italy," *Acta Geophysica*, vol. 59, no. 3, pp. 618–632, 2011.

[11] S. Gambino, G. Falzone, A. Ferro, and G. Laudani, "Volcanic processes detected by tiltmeters: a review of experience on Sicilian volcanoes," *Journal of Volcanology and Geothermal Research*, vol. 271, pp. 43–54, 2014.

[12] W. F. Miller, R. J. Geller, and S. Stein, "Use of a bubble tiltmeter as a horizontal seismometer," *Geophysical Journal of the Royal Astronomical Society*, vol. 54, no. 3, pp. 661–668, 1978.

[13] N. Fournier, A. D. Jolly, and C. Miller, "Ghost tilt signal during transient ground surface deformation events: insights from the September 3, 2010 Mw7.1 Darfield earthquake, New Zealand," *Geophysical Research Letters*, vol. 38, no. 16, article L16305, 2011.

[14] K. Anderson, M. Lisowski, and P. Segall, "Cyclic ground tilt associated with the 2004–2008 eruption of Mount St. Helens,"

Journal of Geophysical Research: Solid Earth, vol. 115, no. B11, article B11201, 2010.

[15] P. P. Firstov, E. O. Makarov, V. E. Glukhov, N. N. Titkov, N. A. Zharinov, and H. Takahashi, "Tilt observations on the Kamchatka Peninsula in 2012–2016," *Seismic Instruments*, vol. 57, no. 4, pp. 424–437, 2021.

[16] S. Gambino and L. Cammarata, "Tilt measurements on volcanoes: more than a hundred years of recordings," *Italian Journal of Geosciences*, vol. 136, no. 2, pp. 275–295, 2017.

[17] D. Dzurisin, *Volcano Deformation: New Geodetic Monitoring Techniques*, Springer Praxis, London, 2007.

[18] S. Gambino, "Tilt offset associated with local seismicity: the Mt. Etna January 9, 2001 seismic swarm," *Open Geosciences*, vol. 8, no. 1, pp. 514–522, 2016.

[19] D. P. Hill, M. J. S. Johnston, J. O. Langbein, and R. Bilham, "Response of Long Valley Caldera to the $M_w = 7.3$ Landers, California, earthquake," *Journal of Geophysical Research: Solid Earth*, vol. 100, no. B7, pp. 12985–13005, 1995.

[20] S. McHugh and M. J. S. Johnston, "An analysis of coseismic tilt changes from an array in Central California," *Journal of Geophysical Research*, vol. 82, no. 36, pp. 5692–5698, 1977.

[21] R. Mellors, J. L. Chatelain, B. L. Isacks, G. Hade, M. Bevis, and M. Prevot, "A tilt and seismicity episode in the New Hebrides (Vanuatu) island arc," *Journal of Geophysical Research*, vol. 96, no. B10, pp. 16535–16546, 1991.

[22] D. Dzurisin, "Electronic tiltmeters for volcano monitoring: lessons from Mount St. Helens," in *monitoring volcanoes: techniques and strategies by the staff of the Cascades observatory, 1980-90*, J. W. Ewert and D. A. Swanson, Eds., pp. 69–83, U.S.G.S. Book, 1992.

[23] G. L. Cooper, *Autonetics Technical Report for Guidance, Control and Flight Mechanics Conference of AIAA*, Autonetics Anaheim, CA, 1970.

[24] J. A. Westphal, M. A. Carr, W. F. Miller, and D. Dzurisin, "Expendable bubble tiltmeter for geophysical monitoring," *Review of Scientific Instruments*, vol. 54, no. 4, pp. 415–418, 1983.

[25] A. Bonaccorso and S. Gambino, "Impulsive tilt variations on Mount Etna volcano (1990–1993)," *Tectonophysics*, vol. 270, no. 1-2, pp. 115–125, 1997.

[26] A. Bonaccorso, A. Bonforte, and S. Gambino, "Twenty-five years of continuous borehole tilt and vertical displacement data at Mount Etna: insights on long-term volcanic dynamics," *Geophysical Research Letters*, vol. 42, no. 23, 2015.

[27] S. Gambino, O. Campisi, G. Falzone et al., "Tilt measurements at Vulcano Island," *Annals of Geophysics*, vol. 50, pp. 233–247, 2007.

[28] S. Gambino, M. Aloisi, G. Di Grazia, G. Falzone, A. Ferro, and G. Laudani, "Ground deformation detected by permanent tiltmeters on Mt. Etna summit: the August 23-26, 2018, Strombolian and effusive activity case," *International Journal of Geophysics*, vol. 2019, Article ID 1909087, 10 pages, 2019.

[29] S. Alparone, A. Bonforte, S. Gambino et al., "Characterization of an active fault through a multiparametric investigation: the Trecastagni Fault and its relationship with the dynamics of Mt. Etna volcano (Sicily, Italy)," *Remote Sensing*, vol. 14, no. 19, p. 4760, 2022.

[30] A. K. Farrell, S. R. McNutt, and G. Thompson, "Seismic attenuation, time delays, and raypath bending of teleseisms beneath Uturuncu volcano, Bolivia," *Geosphere*, vol. 13, no. 3, pp. 699–722, 2017.

[31] A. Douglas, J. A. Hudson, and C. Blarney, "A quantitative evaluation of seismic signals at teleseismic distances-III. Computed P and Rayleigh wave seismograms," *Geophysical Journal International*, vol. 28, no. 4, pp. 385–410, 1972.

[32] D. C. Agnew, "Strainmeters and tiltmeters," *Reviews of Geophysics*, vol. 24, no. 3, pp. 579–624, 1986.

[33] A. Cannata, M. Hellweg, G. di Grazia et al., "Long period and very long period events at Mt. Etna volcano: characteristics, variability and causality, and implications for their sources," *Journal of Volcanology and Geothermal Research*, vol. 187, no. 3-4, pp. 227–249, 2009.